

FIG. 2. The relative volume (dashed curve) and entropy change (solid curve) upon melting as a function of the melting temperature.

The accuracy of Simon's equation<sup>2</sup>

$$P_m = a[(T_m/T_0)^c - 1]$$

is also illustrated in Table I.  $T_0$  is the triple point of argon. The constants  $a$  and  $c$  are both determined from a fit to the melting data at low pressure.<sup>13,14</sup> The results given in Table I show that the large extrapolation to high pressure is exceedingly sensitive to the fit at low pressures.

Finally, the Monte Carlo data indicate the absence of a solid-fluid critical point. Figure 2 shows that the volume and entropy changes upon melting approach an asymptotic limit at high pressures. These and further details will be published elsewhere.

\*Work performed under the auspices of the U. S. Atomic Energy Commission.

<sup>1</sup>F. A. Lindemann, *Physik. Z.* **11**, 609 (1910).

<sup>2</sup>F. Simon and G. Glatzel, *Z. Anorg. Allgem. Chem.* **178**, 309 (1929).

<sup>3</sup>N. Metropolis, A. W. Rosenbluth, M. N. Rosenbluth, A. H. Teller, and E. Teller, *J. Chem. Phys.* **21**, 1087 (1953); W. W. Wood and F. R. Parker, *J. Chem. Phys.* **27**, 720 (1957).

<sup>4</sup>W. van Witzenburg, thesis, University of Toronto, 1963 (unpublished).

<sup>5</sup>A. Michels, J. M. Levelt, and W. de Graaff, *Physica* **24**, 659 (1958).

<sup>6</sup>M. Ross and B. J. Alder, to be published.

<sup>7</sup>M. van Thiel and B. J. Alder, *J. Chem. Phys.* **44**, 1056 (1966).

<sup>8</sup>I. Amdur, J. E. Jordan, and R. R. Bertrand, in Proceedings of the Third International Conference on the Physics of Electronic and Atomic Collisions, University College, London, England, 22-26 July 1963, edited by M. R. C. McDowell (North-Holland Publishing Company, Amsterdam, 1964).

<sup>9</sup>A. A. Abrahamson, *Phys. Rev.* **130**, 693 (1963).

<sup>10</sup>B. J. Alder and T. E. Wainwright, *J. Chem. Phys.* **33**, 1439 (1960).

<sup>11</sup>B. J. Alder and T. E. Wainwright, *Phys. Rev.* **127**, 359 (1962).

<sup>12</sup>E. A. Kraut and G. C. Kennedy, *Phys. Rev. Letters* **16**, 608 (1966).

<sup>13</sup>P. H. Lahr and W. G. Eversole, *J. Chem. Eng. Data* **7**, 43 (1962).

<sup>14</sup>A. Michels and C. Prins, *Physica* **28**, 101 (1962).

## DISPERSION RELATION OF ION WAVES IN MERCURY-VAPOR DISCHARGES

H. Tanaca, M. Koganei, and A. Hirose

Institute of Materials Science and Engineering, Yokohama National University, Yokohama, Japan

(Received 28 April 1966)

The existence of ion acoustic waves externally or spontaneously excited has been discussed by several authors.<sup>1</sup> In addition, ion plasma oscillation has also been observed<sup>2</sup> but without distinguishing it from the potential minimum oscillation. However, the dispersion relation of ion waves covering the whole range of frequency has not been examined. In the present note, experimental confirmation of the dispersion of ion waves in mercury-vapor discharges is reported. The long-wavelength limit is the

ion acoustic wave, and the short-wavelength cutoff is observed at about  $2\pi$  times the Debye length  $\lambda_D$ .

A cylindrical discharge tube (3 cm in diameter) of the hot cathode type is used with two movable grids, each composed of eight thin tungsten spokes in the form of an asterisk. The second grid is operated as the anode at room temperature with discharge currents of 3-30 mA. The first grid, nearer the cathode, is at the floating potential unconnected with

any external emf. Ion acoustic waves spontaneously excited in the discharge are observed satisfying the resonance condition  $f_n \times nL/2 = V_s$ , where  $L$  is the distance between the grids,  $V_s$  is the constant ion acoustic wave velocity, and  $n = 2, 4, 6, \dots$  is the mode number. It should be mentioned that the wavelength of the ion acoustic wave is directly measured by phase-sensitive detection of the light-intensity fluctuations along the tube by a photomultiplier.<sup>3</sup> The wave velocity  $V_s$  thus determined is  $(0.70-0.75) \times 10^5$  cm/sec.<sup>4</sup>

Thus far, we have described our experiments on ion acoustic waves only. In order to examine the dispersion of the waves extending from the ion acoustic to ion plasma oscillations, we carried out spectral analysis of the ion waves between the grids mentioned above, using a panoramic frequency analyzer. An example of the frequency spectrum is given in Fig. 1. The nearly equal distance between the neighboring components in the low-frequency region is found to be independent of the discharge currents and is inversely proportional to the distance between the grids, confirming resonant self-excitation of ion acoustic waves of constant velocity. In the high-frequency region, however, the frequency separation becomes smaller and smaller, indicating a decrease of wave velocity which is discussed below.

The amplitude of the high-frequency components eventually decreases, and it is remarkable that there exists a cutoff beyond which no overtones are observed. The cutoff frequency increases with the square root of the discharge currents,  $\omega_{cut} \propto I_d^{1/2}$ , as illustrated in Fig. 2.

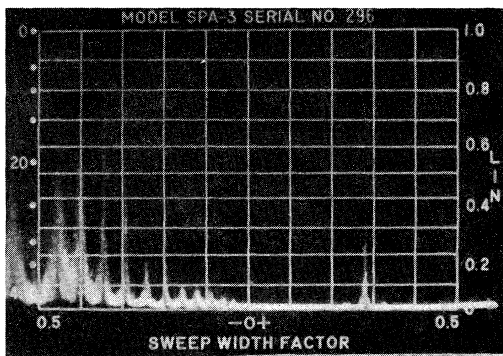


FIG. 1. An example of the frequency spectra of the anode potentials. The full scale is 0-1.0 Mc/sec. The fundamental frequency is 50 kc/sec. The ion plasma oscillation appears at 780 kc/sec.

At a higher frequency beyond the cutoff (Figs. 1 and 2), a large oscillation of definite frequency appears which may be regarded as the ion plasma oscillation because it is proportional to the square root of the current. This frequency is also observed to be about  $(m_e/m_i)^{1/2} \sim 1/600$  of the electron plasma frequency detected at the same time. Though we cannot definitely distinguish it from the potential-minimum oscillation, we use it as the basis for determining plasma density, which implies  $\omega_{pi} = (4\pi ne^2/m_i)^{1/2}$

Neglecting the ion-temperature effect, we may write the ion-wave dispersion relation as

$$\omega^2 = \frac{V_s^2 k^2}{1 + V_s^2 k^2 / \omega_{pi}^2}, \tag{1}$$

where  $V_s = (\gamma k T_e / m_i)^{1/2}$  is the ion acoustic wave

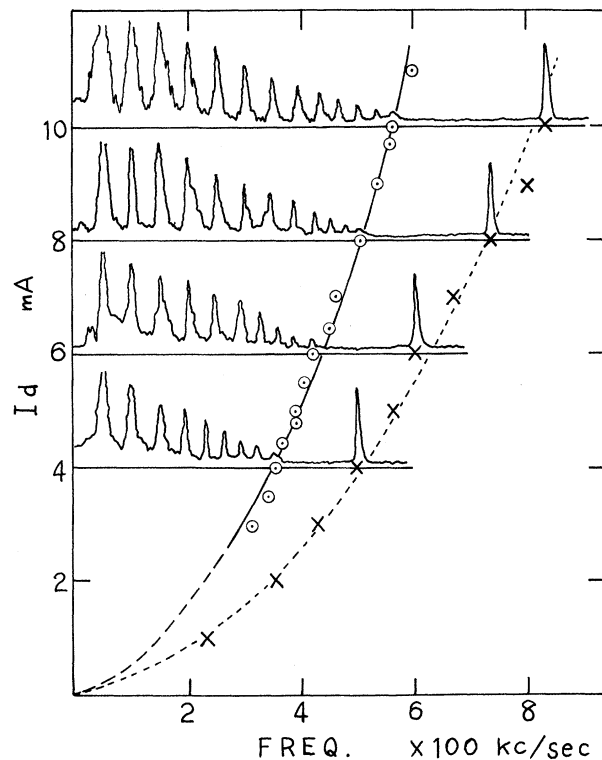


FIG. 2. The cutoff frequency (the final frequency component observed),  $\odot$ , and the ion plasma frequency,  $\times$ , against the current. Both frequencies are proportional to the square root of the current. The reference curves are based on calculation. The frequency spectra also are schematically illustrated for currents of 4, 6, 8, and 10 mA. The ion acoustic velocity is  $V_s = 50 \text{ kc/sec} \times (2.0-0.5) \text{ cm} = 0.75 \times 10^5 \text{ cm/sec}$ , where 2.0 cm is the electrode distance  $L$  and 0.5 cm the sheath thickness.

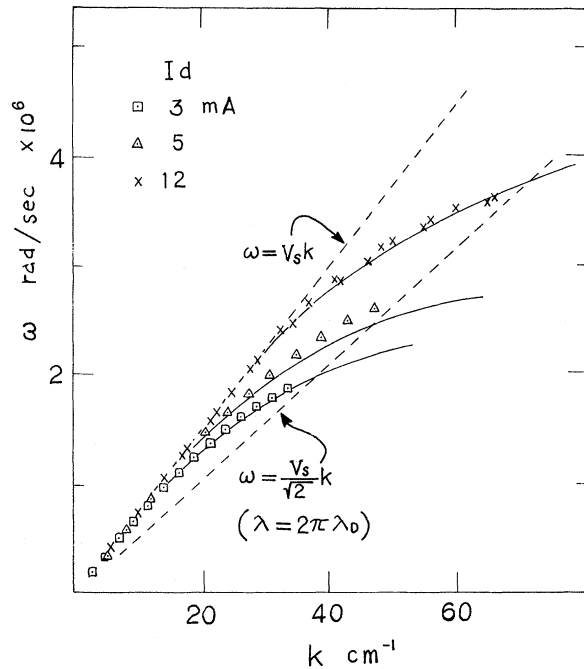


FIG. 3. The  $k$ - $\omega$  diagram of ion waves at currents of 3, 5, and 12 mA. The curves are based on the dispersion relation (1) where the observed ion plasma frequency is used at the respective currents. The cutoff frequency lies on the curve  $\omega/k = V_s/\sqrt{2}$ , independent of the current. In terms of the wavelength, the cutoff occurs at  $\lambda = 2\pi\lambda_D$  at the respective currents.

velocity. A few examples of the spectrum analysis of the waves in the  $k$ - $\omega$  diagram are shown in Fig. 3. It should be emphasized that in our experiment the wavelength is, in the first place, directly measured in order to avoid any ambiguity<sup>5</sup> in assignment of the wave number  $k$  to the component frequencies. The curves are based on the relation (1) where the observed ion plasma frequency is inserted into  $\omega_{p_i}$  at the respective currents. In the low-frequency region the waves have nearly the constant phase velocity of the ion acoustic waves, and in the high-frequency region the velocity decreases gradually in good agreement with the above dispersion relation. The sheath correction<sup>6</sup> is already taken into account in Fig. 3. The ion acoustic wave velocity of  $0.75 \times 10^5$  cm/sec corresponds to the effective electron temperature

$\gamma k T_e \sim 1.3$  eV in rough agreement with Langmuir probe measurements.

The cutoff frequency  $\omega_{\text{cut}}$  and the ion frequency  $\omega_{p_i}$  have the same dependence on current, and are closely related to each other by  $\omega_{\text{cut}} = \omega_{p_i}/\sqrt{2}$  (Fig. 2). The cutoff frequency is determined by the plasma density, and the cutoff points in the  $k$ - $\omega$  diagram are on the straight line  $\omega/k = V_s/\sqrt{2}$  (Fig. 3). In terms of the wavelength, the relation  $\omega_{\text{cut}}\lambda_D = V_s/\sqrt{2}$  is derived from the dispersion relation (1) if  $\omega_{\text{cut}} = \omega_{p_i}/\sqrt{2}$  is satisfied, where  $\lambda_D$  should be defined as  $\lambda_D = (\gamma k T_e / 4\pi n e^2)^{1/2}$ . It is very interesting to observe that the cutoff occurs at the length  $2\pi\lambda_D$ ,  $2\pi$  times the effective Debye length  $\lambda_D$ , in each state of the plasma. (In our notation, the effective electron temperature  $\gamma k T_e$  is used without specifying specific-heat ratio  $\gamma$ .) The cutoff wavelength might be of the order of the shielding length, but the details are still unknown.<sup>7</sup> The excitation mechanism of the ion waves is under examination.

We wish to thank Professor K. Takayama for his kind hospitality in the noise-spectrum laboratory in the Institute of Plasma Physics, Nagoya University.

<sup>1</sup>F. W. Crawford and R. J. Muhler, in Proceedings of the Seventh International Conference on Phenomena in Ionized Gases, Belgrade, Yugoslavia, August 1965 (to be published).

<sup>2</sup>K. Kojima, K. Kato, T. Kawabe, and K. Ogawa, J. Phys. Soc. Japan **18**, 1553 (1963).

<sup>3</sup>A. Hirose, M. Koganei, and H. Tanaca, J. Phys. Soc. Japan **21**, 806 (1966).

<sup>4</sup>H. Tanaca and M. Hagi, Phys. Fluids **9**, 222 (1966). In this note, the wavelength was measured indirectly, assuming waves of mode number  $n = 1, 2, 3, \dots$  instead of  $n = 2, 4, 6, \dots$ . So the velocity must be corrected with a factor  $\frac{1}{2}$ , that is,  $V_s = \frac{1}{2} \times 1.55 \times 10^5$  cm/sec =  $0.78 \times 10^5$  cm/sec. The discussion on the reflection of waves also must be changed.

<sup>5</sup>T. Itoh, J. Phys. Soc. Japan **18**, 286 (1963).

<sup>6</sup>I. Alexeff and W. D. Jones, Phys. Rev. Letters **15**, 286 (1965).

<sup>7</sup>T. H. Stix, *The Theory of Plasma Waves* (McGraw-Hill Book Company, Inc., New York, 1962); B. Anderson and P. Weissglass, Phys. Fluids **9**, 271 (1966); I. Alexeff and W. D. Jones, Bull. Am. Phys. Soc. **10**, 509 (1965).

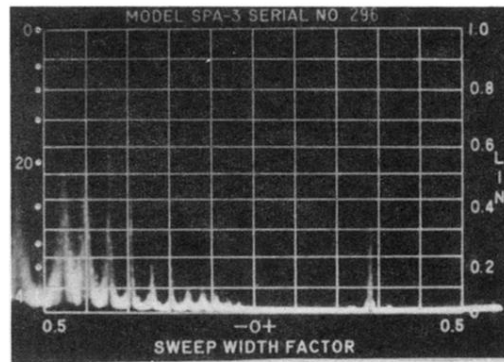


FIG. 1. An example of the frequency spectra of the anode potentials. The full scale is 0-1.0 Mc/sec. The fundamental frequency is 50 kc/sec. The ion plasma oscillation appears at 780 kc/sec.